Fermi National Accelerator Laboratory

FERMILAB-79/43-EXP
7850.507

MODULATION OF NUCLEAR INTERACTIONS USING CHANNELING AT MULTI-HUNDRED GeV ENERGIES

R. A. Carrigan, Jr., B. L. Chrisman, and T. E. Toohig
Fermi National Accelerator Laboratory
Batavia, Illinois 60510 USA

and

W. M. Gibson, Ick-Joh Kim, and C. R. Sun
State University of New York
Albany, New York 12222 USA

and

Z. Guzik, T. S. Nigmanov, E. N. Tsyganov,
and A. S. Vodopianov
Joint Institute for Nuclear Research
Dubna, USSR

and

M. A. Hasan, A. S. Kanofsky, and R. Allen
Lehigh University
Bethlehem, Pennsylvania 18015 USA

and

J. Kubic, D. H. Stork, and A. B. Watson
University of California
Los Angeles, California 90024 USA

June 1979

MODULATION OF NUCLEAR INTERACTIONS USING CHANNELING AT MULTI-HUNDRED GeV ENERGIES

R. A. Carrigan, Jr., B. L. Chrisman, and T. E. Toohig
Fermi National Accelerator Laboratory
Batavia, Illinois 60510

and

W. M. Gibson, Ick-Joh Kim and C. R. Sun
State University of New York
Albany, New York 12222

and

Z. Guzik,* T. S. Nigmanov, E. N. Tsyganov, and A. S. Vodopianov
Joint Institute for Nuclear Research
Dubna, U.S.S.R.

and

M. A. Hasan, A. S. Kanofsky, and R. Allen
Lehigh University†
Bethlehem, Pennsylvania 18015

and

J. Kubic, D. H. Stork, and A. B. Watson
University of California
Los Angeles, California 90024

ABSTRACT

Channeling of protons and positive and negative pions has been observed in a single crystal of germanium at beam momenta of 35, 100, and 250 GeV/c. Both energy loss and scattering have been measured. The channeling effects agree with observations at lower energies suitably scaled to these high energies. The suppression of inelastic nuclear interactions has been directly observed by monitoring multiple track events.

I. INTRODUCTION

In the last several years there has been active interest in the possibility of using single crystals for high-energy physics experiments. While oriented single crystals have been used for many years to obtain polarized bremsstrahlung beams at high energies, it is only recently that the possibility of using techniques similar to those employed in channeling studies at much lower energies for nuclear physics has been raised. G. Temmer[1] has proposed that blocking techniques be used to study particle lifetimes in the same spirit that they have been used to study nuclear isomer states at MeV energies. This type of measurement could be applied, for example, to the study of the η lifetime.[2] Carrigan[3] has suggested that oriented single crystals could be used to study a process called production channeling in which well collimated production processes are used to generate short-lived particles to study their nuclear interactions. Tsyganov,[4] along with others,[5] noted that particles such as electrons moving in single crystals could emit synchrotron radiation which might be used to tag the particles. Tsyganov has also speculated on the possibility of bending and cooling particle beams using channeling. Any of these effects, if observed experimentally, could have interesting applications in high-energy physics.

There is no apparent reason why normal particle channeling should not occur at the highest accelerator energies now available. A beautiful series of experiments by an Aarhus-CERN group[5] has already demonstrated channeling in the 1-15 GeV region. There are, however, a number of problems associated with carrying out channeling studies at very high energies. For example, the mosaic effects in typical single crystals that have been used for polarized bremsstrahlung high-energy experiments are such that the random plane directions can vary by the order of 50 microradians. It may also be difficult to prepare and mount a crystal in such a way that irregularities are not introduced at a level of microradians. There is also a problem in orienting a crystal within the narrow angular region required for channeling studies in the multi-hundred-GeV region. Finally, high-energy experimental techniques are substantially different than those used for most nuclear physics experiments. Beam spills are different and the technology involved can be more complex. Since the additional complex technique associated with the oriented crystal in this multi-hundred-GeV environment is difficult it was felt desirable to carry out a systematic investigation of particle channeling up to the highest available energies before considering in detail possible applications to high-energy physics problems. In addition, there are good reasons to carry out such measurements in terms of the physics associated with the particle channeling process. For example, reduced influence of multiple scattering effects at high energy, elucidation of energy loss of relativistic particles and tests of energy scaling of channeling theory all justify such studies.

In view of these considerations we undertook to investigate channeling effects up to energies of 250 GeV.

The orientation of a single crystal affects several different phenomena that occur in the crystal. The geometrical channeling effects are characterized by a critical angle beyond which the particles tend to move out of channeled trajectories. For highly relativistic energies the axial critical angle is given by

$$\psi = \alpha\sqrt{\frac{4Ze^2}{pcd}}, \qquad (1)$$

where Z is the atomic charge of the target nucleus, d is the atomic spacing along the lattice string, p is the momentum and is a constant of the order of unity whose precise value depends on the thermal vibration amplitude of the crystal atoms. At high energy this critical angle is small, typically on the order of 40 microradians for 250 GeV/c for positive particles axially channelled along the < 110 > axis in germanium. Particles incident parallel to a crystal axis show substantially less energy loss because of the reduction of close ionizing collisions. Angular distributions upon emergence from the crystal for particles incident in the vicinity or less than the critical angle with respect to the axes or planes can also be substantially modified. Finally, particles in channeled trajectories are dechanneled by a variety of effects. These determine an upper limit on the thickness of the crystal that will give strong channeling effects at a particular energy.

This article covers the effects of the channeling process on close collisions and nuclear interactions. The experimental arrangement is reviewed in some detail in Sec. II to facilitate these discussions. In Sec. III, the physical mechanisms for the modulation of collisions and near collisions are discussed. Section IV discusses large angle scattering: Section V discusses large energy loss, and Section VI deals with multiple-track events. Other articles will discuss geometrical effects near the crystal axis including "donuts," energy loss in more detail, and planar effects.

II. EXPERIMENT

In this experiment, channeling effects were measured in a germanium crystal. High-energy particles in the M1 beam line of the Meson Laboratory at Fermilab were directed at the crystal. The incident and exiting angles of each particle relative to the crystal were precisely measured by a set of high-resolution drift chambers. The energy loss was measured by the germanium crystal operating as an intrinsic solid state detector. Figure 1 shows a schematic diagram of the experimental apparatus. This arrangement follows that originally employed in channeling experiments carried out at CERN.[6]

The hyperpure germanium crystal was mounted in a vacuum goniometer with polar and azimuthal degrees of angular freedom relative to the beam. The goniometer was remotely controlled and could be stepped in 20 microradian increments. The germanium crystal was configured so that it acted as a transverse-field intrinsic detector capable of measuring the energy deposited in the crystal.[7] This required that the crystal be cooled to near liquid nitrogen temperature with a moveable cold-finger. Using x-ray alignment the crystal was fabricated so that a < 110 > axis was perpendicular to each of two faces of the crystal to within two degrees. The thickness along one < 110 > axis was one centimeter while it was two centimeters in the other direction. Although alternate orientations of the crystal could be used to study the effect of the crystal thickness on dechanneling, all of the running reported here was with a crystal thickness along the beam of 2 cm. In the third direction the crystal was 0.8 cm thick. The crystal voltage was set high enough so that it was fully depleted. Most of the running was with 500 volts on the crystal.

The system was triggered by a coincidence in three upstream beam counters in addition to scintillation counters T1 and T2 shown in Fig. 1. Pulse height discrimination of an upstream counter vetoed the trigger if two particles arrived within an rf bucket. A veto was also produced if a second particle was detected within the period from 500 ns before to 80 ns after the trigger particle. T1 was placed so as to define the beam to be on only one side of the principal drift wires to eliminate left-right ambiguities. An anti-counter with a hole in it smaller than the crystal was placed so that the hole was centered on and partially covered the crystal. This assured that any particle not triggering the anti had gone through the crystal. The signal from the germanium crystal was fed into a conventional nuclear linear electronics amplifier system operating with a rise time of 7 microseconds. This was sent in turn to an ADC readout by both an on-line HP2000 computer and a pulse-height analyzer. The detector system was calibrated using gamma-ray sources. The typical resolution for the detector on the Na^{22} line was 10 keV (rms).

The particles passing through the crystal were detected with a calibrated drift chamber system that had been used immediately prior to these channeling measurements for a measurement of the pion and kaon form factors at Fermilab. The incident directions of the particles in the beam were measured in two drift-chamber modules placed upstream of the detector and spaced 30 meters apart. The second module was about 1 meter upstream of the single crystal. An additional drift chamber module was located 17 meters downstream of the detector. Each module contained drift chambers for four horizontal and four vertical measurements. Care was taken to reduce the sources of multiple scattering. The rms spatial resolution per module was on the order of 90 microns. Measurements were also made with the crystal removed from the system to measure the angular resolution of the apparatus. At 35 GeV/c the width of the projected deflection angle distribution with no crystal was 46 microradians rms. The rms distribution at 250 GeV with the crystal removed was 10 microradians. This distribution is some measure of the angular resolution of the system. At 250 GeV/c much of the width of that distribution was due to the spatial resolution of the drift planes, while at 35 GeV/c most of the width was due to multiple scattering in the system. Figure 2 shows the predicted and observed experimental resolution as a function of momentum. The momentum dependences of the resolution functions behaved essentially in the way expected. (It should be noted that the system resolution is different for each of three angles: the incident angle, the exit angle, and the scattering angle. This is because different sets of quantities enter in the measurement of each angle and the incident and outgoing angles are not sensitive to multiple scattering.) The observed experimental resolution for scattering angles measured with the crystal removed is in good agreement with the predicted resolution. The resolution of the apparatus was sufficient to clearly determine the angular spread of the axial channeling effects. Planar widths are about a factor of 1/3 those of the axial widths so that the magnitudes of the planar effects would be more affected by resolution; however, planar channeling was easily observed. The system performance is also indicated in Fig. 2 by the measured width of the outgoing < 110 > axial transmission peak with a selection on small scattering angles and small energy losses. The Aarhus-CERN measurements[9] are extrapolated from 1.35 GeV/c using $1/\sqrt{p}$. The effects of resolution have not been removed for either experiment. The agreement between the measurements is good. In addition, it is clear that the apparatus has achieved the high resolution required for experimental measurements at high energies.

In view of the extreme precision and resolution required to measure angles on the order of tens of microradians it is not surprising that some problems were encountered. Two were significant enough to require some consideration. From run to run the crystal axis as seen by the drift-plane system appeared to wander, drifting as much as thirty microradians over the time period during which the data were taken for one energy. Figure 3 shows a characteristic drift during the 250-GeV data collection. There is some indication that this wander was due to thermal cycling of the goniometer as the level of liquid nitrogen in the reservoir changed since some of the largest changes seemed to be correlated with nitrogen fill times for the dewar. We have inferred that the crystal axis wandered since the apparent crystal axis as seen in the incident and exit plane systems tracked each other. We cannot rule out some contribution from motion of the drift-chamber mounts. For the results reported here the apparent axial drift was factored out by making a coordinate transformation to align the crystal axis for all runs.

The second problem was associated with a slight non-linearity of the drift behavior in the chambers. A somewhat similar pattern was observed in the kaon form-factor experiment. Each coordinate could be determined from a left and right wire. Near the edge of the drift region these two coordinates could differ by several hundred microns. Over the middle 50% of a chamber this difference averaged much less than 50 microns. The bulk of the data was taken in the region centered between the wires. For the data reported here no correction was made beyond averaging the left and right coordinates.

The experiment was performed in the M1 beam of the Meson Area at Fermilab. For this experiment the peak momentum was 250 GeV/c, the highest momentum used in the kaon form-factor experiment. In addition, 100 GeV/c and 35 GeV/c momenta were used; 35 GeV/c was the lowest beam momentum with tuning parameters already established for the beam. We planned, thereby, to link more closely to the highest energy CERN data at 17 GeV. The beam line was equipped with a differential Cerenkov counter to distinguish particle types during part of the run. This counter was not in operation for all phases of the experiment. Typical angular divergences for the beam ran from 50 to 275 microradians. For positive beams at 250 GeV/c the beam was typically 92% to 95% protons. At 35 GeV/c greater than 85% of the beam was pions for both positive and negative polarities.

The M1 beam is capable of rates of up to several million particles per pulse. For the channeling experiment, we were interested in running at as high a rate as possible. While each particle passing through the germanium crystal shed some light on channeling questions, it often proved desirable to select on the incident beam direction so that it was possible to test on a very narrow range of incident angles. For this it has been useful to have the best possible statistics available. Initially, it appeared that the store time for the on-line computer used for the form-factor measurements would be the main limitation on rate. Based on that, a preprocessor was incorporated into the electronics. This preprocessor was able to identify small or large deflections in projected angle in about 80 microseconds and decide whether or not to make the store into the computer. By cutting out the time-consuming store, many more events could be measured with a certain characteristic angular deflection. However, by limiting the number of wires used in the drift planes it was found that the computer could store several hundred events per pulse. In practice the rate was limited by the crystal linear electronics to approximatley 300 computer triggers per pulse corresponding to beam intensities of 20K/s. For nearly all of the running the preprocessor was used only as an auxiliary tag rather than a device to trigger computer store operation.

The crystal was oriented by looking at the ratio of small energy loss events relative to all events as the crystal orientation was varied. Near planes and axes this ratio increased. Typically this alignment process required many hours. When the < 110 > axis was found, it was oriented along the beam direction. The beam angular divergence was such that the crystal could be bathed in a range of particle directions that extended well beyond the solid angle covered by the axial channeling effects.

The trajectories for all particles passing through the crystal and the digitized pulse height corresponding to energy loss were stored on tape by the computer. In addition, an on-line program was used to find and display the incident, exiting, and scattering angles for a random subset (~25%) of the particles. The on-line displays were useful for checking channeling geometries and making sure they were adequately illuminated by the beam. The results reported in the article are from a full off-line analysis of all of the events.

The analysis proceeded by plotting two dimensional histograms of the incident and exiting particle distributions selected on various features such as energy deposit in the crystal. Characteristically incident distributions were normalized by dividing them by the incident distribution with no selection on the data. Information from the kaon form factor experiment and straight-through - no crystal events was used to calibrate the drift-chamber system.

III. SUPPRESSION OF COLLISIONS AND NEAR COLLISIONS

Central to some of the possible applications of channeling at high energy is the suppression or enhancement of nuclear interactions along channeled directions. For example, the production channeling mechanism suggested by Carrigan[3] relies on enhancing nuclear interactions along a crystal axis.

Several types of collisions occur in a crystal lattice: 1) Coulomb collisions with electrons resulting in ionization or excitation of the electrons. A fair fraction of these collisions are with inner electrons. For germanium about half of the energy loss in a random direction is due to excitation of the inner-shell electron. 2) Elastic nuclear scattering can occur. This includes Coulomb scattering from a nucleus or nucleon, elastic scattering due to nuclear forces, and the interference between nuclear and Coulomb scattering. 3) Finally inelastic nuclear collisions can occur.

Each type of collision has a different characterization. In addition, channeling effects for positively or negatively charged particles are fundamentally different. Positive particles are repelled from axial strings while negative particles are attracted to them.

For positive particles channeled along axial directions, ionizing collisions with the inner electron shells are suppressed since positive particles are repelled from nuclear strings and there are fewer near encounters.

Elastic nuclear and some Coulomb collisions are characterized by large scattering angles compared to ordinary multiple scattering. For example, single Coulomb and nuclear scattering occur at about equal magnitudes at an angle of 1000 microradians in germanium for a momentum of 250 GeV/c, while the characteristic multiple scattering angle for a 2-cm thick piece of germanium is 56 microradians. Large scattering angles, then, imply nuclear or large angle Coulomb scattering processes or a combination of both. In an elastic collision the recoiling nucleus also gains energy but in most cases this is quite small. For the case cited above the energy transferred to the nucleus is 0.45 MeV. Since the recoil kinetic energy is small, all of the elastic energy loss can be absorbed in a relatively thin slice of crystal. Anomalously high energy deposit in a crystal can be due in part to this type of collision. The magnitude of this effect relative to the total energy loss depends, of course, on the crystal thickness. Thinner crystals should show more of an effect since the recoil collision contribution can be a relatively larger part of the total energy deposit. Along an axis these collisions are suppressed for positive particles so there should be fewer large energy depositions and large angle collisions. A significant fraction of these elastic collisions are due to Coulomb scattering. There is no direct way to sort out Coulomb collisions from other elastic nuclear processes. On the other hand, the Aarhus-CERN group[11] has studied the angular distribution of scattering events in germanium and has shown that it can be well fitted by a combination of all the effects noted above.

Inelastic nuclear collisions result in the production of nuclear particles from projectile or target fragmentation. Energetic fragments, particularly from projectile fragmentation, can leave the target and be detected downstream. These produced particles can also deposit additional energy during their transit through the crystal.

In the Fermilab channeling experiment the drift-chamber module furthest downstream could be used to detect events with multiple tracks when they were within the angular range subtended by the drift-chamber module. The active chamber size restricted the rate of multiple-track detection. In the present experiments, the system was sensitive to multiple-track events at 250 GeV/c and was severely limited in sensitivity at 35 GeV/c. At 250 GeV/c, then, this technique could be used to directly monitor the modulation of nuclear interactions.

Clearly the suppression of multiple track events along a crystal axis represents direct evidence of the suppression of nuclear interactions since this signature arises in only one way.

IV. LARGE ANGLE SCATTERINGS

Ideally, to demonstrate the effect of crystal orientation on large angle scattering events and particularly those due to nuclear processes, a selection should be made on scattering angles substantially larger than the multiple scattering and critical angles. Near a crystal axis, particle trajectories behave in quite complex ways. In some sense particles moving near an axis preserve angular momentum about that axis. If incident trajectories are selected that lie inside or near the critical angle this results in angular distributions that resemble donuts. Donut effects complicate the angular distribution and can produce angular deflections substantially larger than the critical angle. These effects will be discussed in detail in a subsequent paper.

The size of the apparatus places a constraint on the largest scattering angle that can be measured. With that constraint the minimum angle selection on large angle scatters should be made as large as practical. For example, at 100 GeV/c scatters were selected that were 250 microradians or greater. That corresponds to 3.7 times the critical angle and 1.8 times the rms multiple scattering angle. At these scattering angles multiple scattering as contrasted with nuclear scatterng from coulombic or nuclear processes still produced a substantial portion of the recorded events. Note, however, that for channeled particles the normal effect of multiple scattering is also suppresed.

Figure 4 shows the normalized incident angle distributions for 250 GeV/c mixed, positive particles. These distributions are found by dividing the incident angular distribution after a selection on scattering angles greater than some angle by the unselected angular distribution. The distributions are taken relative to the crystal axis. The curves have a deep dip at the axis, indicating that large angle scatters are suppressed near the crystal axis. At angles away from the axis the probability of a scatter increases significantly. This peak is due to donut effects. Further out the scattering drops off. This probability is set by multiple or nuclear scattering in a random direction and the efficiency for detecting large angle scattering events. The levels at large angles are approximately correct on that basis. As the selection angle increases from 50 microradians to 300 microradians the overall distribution is lowered and the minimum becomes almost zero. The position of the maximum shifts out. Eventually, when the selection angle is five or six times the critical angle, the prominent maximum falls away. This is probably because the donut effect is no longer available as a source to enrich the large angle scattering events. With a selection angle of 300 microradians, five times the projected multiple scattering angle, most of the events are probably due to nuclear interactions. This curve, then, is a direct indication of the suppression of nuclear events.

It is interesting to note that at these high momenta, with the multiple scattering comparable to the critical angle, that near-axis trajectories have significantly increased angular dispersion. Of course within the critical angle large angle scattering decreases significantly. However when the total effect near the axis is taken into account, scattering angles are significantly increased. Thus, near an axis, the crystal is a "super" scatterer.

The measured width of the dip is a function of the selection angle. The half-width of this curve should be related to the critical angle. Although there is some dependence on scattering angle, the half widths relative to random range from 47 to 62 micro-radians for scattering angles greater than 100 microradians. Characteristically the half width relative to random is about one and a quarter times the critical angle. Figure 5 shows the same distribution for 100-GeV mixed, positive particles.

The maximum appears at an angle of two or three times the critical angle. As noted above this arises from 'donut' effects and is not due to the usual compensation shoulders discussed in classical channeling theory and observed for scattering in thin layers at lower energy.

At 250 GeV/c the probability of a large angle scatter near the axis is from 5% to 10% of the probability of such a scatter in a random direction which is comparable to that observed for very thin crystals at lower energy. This indicates little dechanneling at this energy in the two centimeter thick crystal. Dechanneling will increase the minimum yield. At lower energies the dechanneling length decreases. For example at 35 GeV/c the minimum is around 30% of that in a random direction. In the CERN experiments dechanneling comparable to that observed in the 2 cm thick crystal was observed in a 4 mm thick crystal at 15 GeV and at MeV proton energies the same amount of dechanneling is observed in germanium crystals of about 30 microns thickness. This dramatic increase in the dechanneling length at high energies is a consequence of the reduction of multiple scattering angle (which scales 1/pv) relative to the channeling critical angle (which scales as $1/\sqrt{PV}$) as the energy is increased. This effect is one of the primary reasons for carrying out such high energy measurements. The apparently small amount of dechanneling in the 250 GeV/c and 100 GeV/c data will be particularly important in considering transmitted particle (or donut) results to be reported in a subsequent paper.

Figure 6 shows the distribution for positive and negative pions at 35 GeV/c. The selection angle is 300 microradians, roughly three times the critical angle. However, the projected multiple scattering angle is now 400 microradians. In view of the acceptance of the downstream plane it is difficult to make the selection angle sufficiently large so that it mainly selects nuclear-interaction events.

There is a distinct difference between the positive and negative particle distributions. The negative particle distribution shows a much shallower minimum that is several times as wide. Since negative particles near an axis are in regions of higher electron density than positive particles, it is logical that there would be less suppression of large scatterings. In the CERN experiment[12] there was a slight suggestion of a sharp peak at angles near the axis. One might expect an enhancement there because of the increased probability of nuclear interactions for negative particles moving close to and parallel to atomic strings. There is no statistical evidence for such a peak in the present results.

V. LARGE ENERGY LOSS

When a positive particle moves near an axis large energy losses are suppressed. The particle travels through regions of low electron density. Nuclear interactions are also suppressed. Negative particles, on the other hand, are free to travel in these forbidden regions so that the fraction of high energy losses remains relatively unchanged.

Both these features were observed in this experiment. Figure 7 shows the fraction of incident positive particles at 250 GeV/c with energy losses greater than 1.5 times the most probable energy loss as a function of the angle from the crystal axis. The half width at half maximum is roughly equal to the critical angle. Above 1.5 times the most probable energy loss the width of the dip seems relatively insensitive to the value of the minimum energy loss used. A large fraction of these collisions are probably due to nuclear interactions. Many of them are associated with multiple hits in the downstream drift-chamber module. This is discussed in more detail in the next section. Note that there is some indication that scattering events with angles two or three times larger than the critical angle, that is those events associated with larger donuts, have a slightly larger fraction of large energy losses. This is an interesting observation for positive particles.

Figure 8 shows the same distribution for positive and negative 35 GeV/c pions. The positive particles show a dip similar to the 250 GeV/c case. On the other hand, the negative case shows no evidence for any dip near the crystal axis and many even indicate a slight enhancement.

VI. MULTIPLE TRACK EVENTS

As noted earlier, inelastic nuclear collisions result in the production of nuclear particles from processes such as projectile or target fragmentation. At high energy the multiplicity of charged particles produced by collisions on hydrogen is given by

$$\langle n_c \rangle = -4.8 + 10/\sqrt{2mp} + 2 \ln (2\,mp), \tag{1}$$

where $\langle n_c \rangle$ is the average charged particle multiplicity, m is the mass of the proton in GeV/c^2 and p is the beam momentum in GeV/c.[13] In the forward direction Busza et al.,[14] find that there is no increase in multiplicity per nuclear interaction in a complex nucleus. At 250 GeV/c the average charged multiplicity is 8 particles per interaction. Simultaneously between three and four

π^o mesons are produced. A typical inelastically produced particle has a transverse momentum of 0.3 GeV/c. At 250 GeV/c incident momentum, with a total multiplicity of about 11, a typical particle angle will therefore be 13 milliradians. This should be compared to the maximum angle of 7.5 milliradians that the downstream drift chamber can detect.

In the Fermilab channeling experiment the drift-chamber module furthest downstream was used to detect events with multiple tracks. This module consisted of four x and four y planes with wires 25-cm long. Each plane had two active sense wires. These wires each detected tracks out to 2.1 cm on either side of the wire. Since all wires were not active, the area covered by x or y wires was a cross with an active arm length of 25 cm. Each succeeding plane was staggered by one wire spacing. A simple multiple track algorithm was used here. If two x wires fired or if two y wires fired after one x wire had fired, the event was recorded as a multiple-track event. Other more complicated algorithms were tried but they had little effect on reducing the background. Most of the background seemed to come from two real tracks passing through the apparatus. This could be seen both by running the same algorithm on the upstream module and by looking at multiple tracks in the downstream module with no germanium target in place. The background rate was about the same under these circumstances and was consistent with the background observed below. The active solid angle for detecting multiple hits in this geometry is approximatley 126 square milliradians. Since the area is quantized there is some probability that all tracks will be in a region that defines a single track. The net effect due to this degradation is to degrade the efficiency to 0.55 of the efficiency of a perfect multi-track detector at 250 GeV/c. It should be noted that the trigger scheme automatically required that at least one track be present in the third module.

The overall efficiency for detecting inelastic nuclear interactions depends on the charged multiplicity of the interaction and the geometrical detection efficiency per particle. Since one particle is required by the trigger the probability of detecting an interaction is

$$E_p = E_g (< n_c > - 1) E_m, \qquad (2)$$

where E_g is the geometrical efficiency, $< n_c >$ is the charged multiplicity, and E_m is the efficiency of the plane system for detecting two or more tracks. The charged-particle multiplicity changes from roughly 5 to 8 as the momentum goes from 35 to 250 GeV/c. The geometrical efficiency per particle depends on the square of the mean angular spread of the charged particles. The mean angular spread scales inversely as the incident momentum so that the geometrical efficiency is proportional to p^2. At 250 GeV/c the geometrical efficiency is about 20%. At 35 GeV/c it is about 1%. As noted earlier E_m is about 0.55. With a charged multiplicity of eight at 250 GeV, this means that an inelastic nuclear interaction, once the system is triggered, will be detected with about 80%

efficiency. At 35 GeV/c less than 3.1% of the inelastic nuclear interactions will be detected in the downstream module once the system is triggered.

With the algorithm described above it is possible to examine the angulár distribution of incident particles that generate multiple tracks. This can be expressed as a normalized fraction of the incident distribution. The distribution is taken relative to the crystal axis. Figure 9 shows this distribution for 250 GeV/c positive particles. The abscissa is the incident angle relative to the crystal axis. There is a clear depression in the distribution along the < 110 > axis of the crystal. The half width at half maximum is 35 microradians. This corresponds to 80% of the critical angle at 250 GeV/c. The change in rate from the random to the aligned direction is 2.2%.

This should correspond approximately to

$$f = f_i \, E_t \, E_p, \tag{3}$$

where f is the fraction of the particles that interact and are detected, f_i is the fraction of the particles that interact, E_t is the efficiency for triggering on an interaction and E_p is the probability for detecting a nuclear interaction with perfect triggering efficiency. For a 2-cm thick crystal, an interaction cross section of 30 mb per nucleon, and a nuclear cross section that goes as $A^{2/3}$, the interaction probability f_i is 4.6%. The trigger efficiency was set by the size and position of the counter just before the third module. This counter was 2.5 in. in diameter. A naive calculation shows that its efficiency would be 25% for detecting a track from a 250 GeV/c interaction. In fact the efficiency could be somewhat higher if the angular distribution of the fragments was properly taken into account. In view of considerations such as this it is quite plausible that E_t could have been the order of 0.6. As noted earlier E_p is 0.8 at 250 GeV/c. The measured value of f was 2.1%. This is quite consistent with the model outlined above.

The contribution along the axis could come from a variety of sources including dechanneling and accidentals. As noted above, accidentals occur when two tracks are present in a module. It was previously noted that provision was made for suppressing two beam tracks in the system using an overlap gate from 500 ns before to 80 ns after the trigger using an upstream counter. Multiple tracks in a particular module could still arise from delta rays, "in" scattering, or particle production outside of the crystal and downstream of the double pulse suppressing counter. One way to measure this contribution was to remove the crystal and measure the rate. The dashed line in Fig. 9 shows this rate. The relative rate of "multiple hits" in the upstream module is also of the same magnitude. This suggests that most of the rate on axis is due to background rather than dechanneling effects. The relative absence of dechanneling in the large angle scattering results noted earlier is consistent with this point of view.

At 100 GeV/c f should be 1/5 as large as at 250GeV/c. This is too small to be measured with any effectiveness. No statistically significant signal was seen; 35 GeV/c is even less favorable and no signal was seen. For this reason it was not possible to measure any effect on the negative 35 GeV/c particles.

It is interesting to compare the efficiency of the Fermilab detector to the CERN detector. Since the half width of the CERN large downstream chamber was 25 cm, the half angle of the downstream module was approximately 32 milliradians. The multiplicity is correspondingly lower at 15 GeV/c. Furthermore, the CERN crystal was 1/5 the thickness of the Fermilab crystal so that interactions would occur 1/5 as frequently. Overall the CERN detector, operating at 15 GeV/c, would have seen a signal of 1/7 the relative magnitude of the Fermilab detector operating at 250 GeV/c. Thus it could have been quite difficult to see multiple events by this technique with the CERN detector.

As noted earlier, the occurrence of a nuclear interaction in the crystal will give rise to an increase of energy deposit in the crystal. This situation is complicated by the fact that target recoil particles are moving slowly and can lose a large amount of energy in the crystal. The relative contribution from this feature is diminished if the crystal is thick so that overall ionization losses are large. For interactions near the upstream end of the crystal the full ionization energy of the eight or so charged particles will be observed. For interactions deeper in the crystal less of the effect of the multiplicity of charged particles will be detected.

For some fraction of the multiple-track events detected in the third plane the energy loss in the crystal should be anomalously large. At 250 GeV/c about half of the multiple-track events above the no-crystal background have energy losses 50% greater than the normal most probable energy loss while for random events this occurs only 8% of the time. About 1/3 of the events have energy losses greater than two times the most probable energy loss. It appears that many of the true multiple-particle events have associated high-energy deposits in the crystal.

VII. DISCUSSION

This experiment has demonstrated that channeling experiments can be extended to the highest energies now available with existing techniques. Crystal stability and detector resolution can be maintained at a level where angular effects on the order of 40 microradians can be readily observed. Crystal axes can be located using standard techniques.

The critical angle scales to these very high energies in accordance with conventional channeling theory.

Multiple scattering and dechanneling are dimished as the energy increases so that thicker crystals can be employed.

Near axes these effects result in an average increase of angular dispersion that becomes quite pronounced, in effect a super-multiple scattering.

For particles incident parallel to the crystal axis these results also clearly show that nuclear interactions are suppressed. This fact raises several interesting possibilities.

For example, this technique could be used to make an electron target. The present experiment used the apparatus employed earlier to measure the kaon form factor. This was done by scattering k mesons on electrons. Kaon scattering from nucleons constituted a background in the experiment. This background could have been suppressed by bringing a parallel beam of kaons into an oriented single crystal aligned along the beam. Some care would have been required to make the beam sufficiently parallel but the idea is certainly an intriguing possibility. The technique would be increasingly effective at higher energies.

We would like to thank the members of the Dubna-Fermilab-Notre Dame-Pittsburgh-UCLA form-factor experiment for letting us use their apparatus and helping to acquaint us with its operation. A. Wehmann and M. Atac have been particularly helpful. We would also like to express our thanks to the Directorate and Staff at Fermilab for permitting us to perform this experiment in conjunction with the form-factor experiment.

REFERENCES

*Now at Institute of Nuclear Research, Swierk, Poland.

†Funded in part under contracts with the U. S. Department of Energy and Lehigh University EY-76-S-02-2894.A002.

[1]G. W. Temmer, Proceedings of the Kentucky Conference on Low-Medium Mass Nuclei, (J. P. Davidson and B. Korn, Eds.), 192, (1973).

[2]H. Nielsen, Aarhus Meson Channeling Meeting, October 1977.

[3]R. A. Carrigan, Jr., Phys. Rev. Lett. 35, 206 (1975).

[4]E. N. Tsyganov, Fermilab Internal Report TM-684, September 8, 1976.

[5]See for example, M. A. Kumakhov, Phys. Lett. 57, 17 (1976), and Phys. Stat. Sol. (b) 84, 41 (77), R. W. Terhune and R. H. Pantell, App. Phys. Lett. 30, 265 (1977).

[6]A number of articles have covered the Aarhus-CERN channeling experiments. See, for example, H. Esbensen et al., Phys. Lett. 72B, 408 (1978), H. Esbensen et al., Nucl. Phys. B127, 281 (1977), H. Esbensen et al., Phys. Rev. B18, 1039 (1978).

[7]The crystal detector was specially fabricated by ORTEC using hyperpure germanium.

[8]T. S. Nigmanov et al., Fermilab Report Fermilab-76/26-EXP, March 1976.

[9]O. Fich, J. A. Golovchenko, K. O. Nielsen, E. Uggerhøj, C. Vraast-Thomsen, G. Charpak, S. Majewski, F. Sauli, and J. P. Ponpon, Phys. Rev. Lett. 36, 1245 (1976).

[10]W. F. Baker et al., Phys. Lett. 51B, 303 (1974).
W. F. Baker et al., Fermilab Report FERMILAB-78/79-EXP, October, 1979.

[11]S. K. Andersen et al., Nucl. Phys. B144, 1 (1978).

[12]Aarhus-CERN group, private communication.

[13]See, for instance, J. Whitmore, Phys. Rep. C10, 273 (1974).

[14]W. Busza et al., Phys. Rev. Lett. 34, 836 (1975).

FIGURE CAPTIONS

Fig. 1: Schematic diagram of high-energy channeling experiment.

Fig. 2: Momentum dependence of the critical angle, resolutions, and the measured half width of the axial transmission line for a selection on small scattering angles and low energy loss. The Aarhus-CERN axial width is extrapolated from 1.35 GeV/c using $1/\sqrt{p}$. The diamonds are the representative measurements for this experiment. Both sets are raw, that is, resolution effects have not been removed. $\Delta\theta$ resolution refers to the expected resolution for measuring a scattering angle while outgoing resolution refers to the resolution for measurement of outgoing angles. The "X"s show the experimental measurements with the crystal removed. All angles except the critical angle are given in terms of half width at half maximum.

Fig. 3: Apparent crystal axial drift for horizontal and vertical projected angle measurement at 250 GeV/c. The horizontal axis is run number. Error flags are the average difference in determining axial direction by two different methods. The lines are visual fits to the points. The data reported in the article have had this apparent drift factored out by making a coordinate transformation to align the crystal axis for all runs.

Fig. 4: Fraction of +250 GeV/c particles scattering through large angles as a function of incident angle relative to the axis. The numbers shown by the curves are the minimum scattering angle in microradians.

Fig. 5: Normalized incident angle distribution for mixed 100 GeV/c positive particles selected for large angle scatterings. The minimum angle is 250 microradians. The distribution is taken relative to the crystal axis. f is the probability for a scatter at an angle θ_r relative to the axis with the selection on minimum angle divided by the probability with no selection.

Fig. 6: Relative behavior of positive and negative particles for a selection on large scattering angles. The graph shows the fraction of 35 GeV/c particles scattering more than 300 microradians as a function of incident angle relative to the axis. The dots are positive particles while the open circles are negative particles.

Fig. 7: Behavior of 250 GeV/c positive particles with energy loss greater than 1.5 times the most probable energy loss. The figure shows the fraction of these particles as a function of incident angle relative to the axis in microradians.

Fig. 8: Relative behavior of 35 GeV/c positive and negative particles with energy losses greater than 1.5 times the most probable energy loss. The figure shows the fraction of these particles as a function of incident angle relative to the axis in microradians.

Fig. 9: Normalized incident angle distribution about crystal axis of particles producing multiple hits in the downstream module at 250 GeV. These correspond, in part, to events in which nuclear interactions occurred. Dashed line shows distribution with crystal removed from system, probably mostly due to beam particles with delta rays. Note the clear reduction of nuclear interactions for particles moving along the crystal axis.

KAON FORM FACTOR APPARATUS
ADAPTED TO HIGH ENERGY CHANNELING

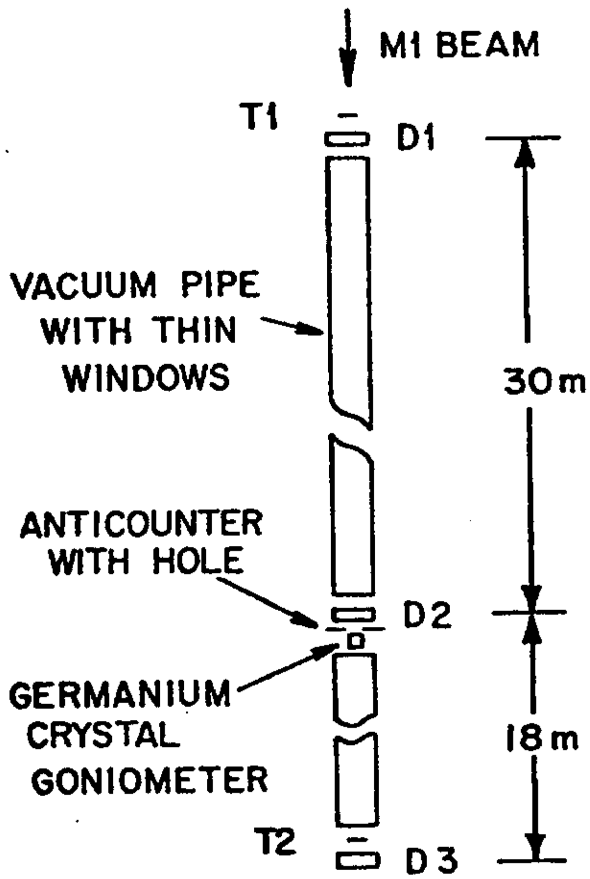

Fig. 1

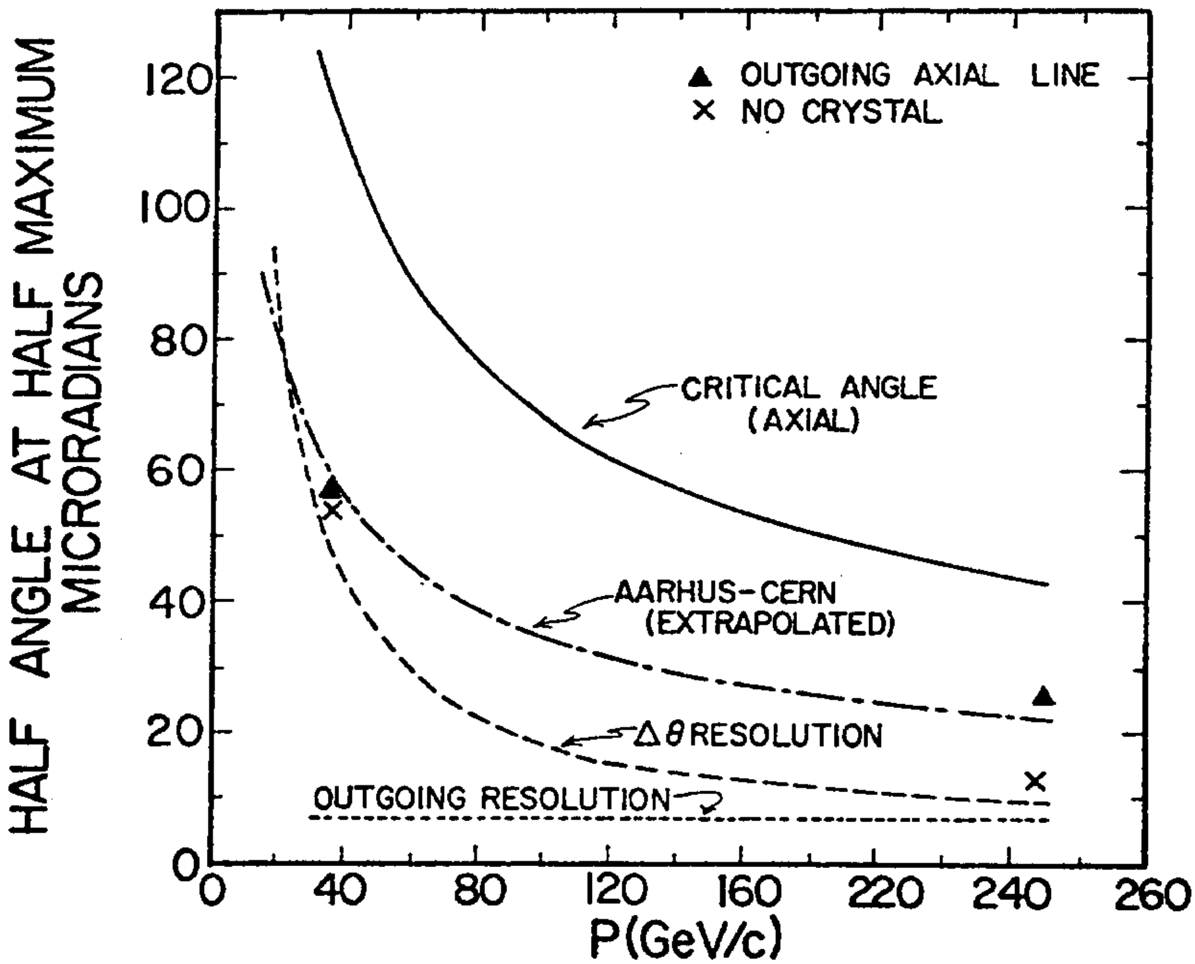
HALF ANGLE AT HALF MAXIMUM
MICRORADIANS
P(GeV/c)
OUTGOING AXIAL LINE
NO CRYSTAL
CRITICAL ANGLE
(AXIAL)
AARHUS-CERN
(EXTRAPOLATED)
Δθ RESOLUTION
OUTGOING RESOLUTION
0
20
40
60
80
100
120
0
40
80
120
160
220
240
260

Fig. 2

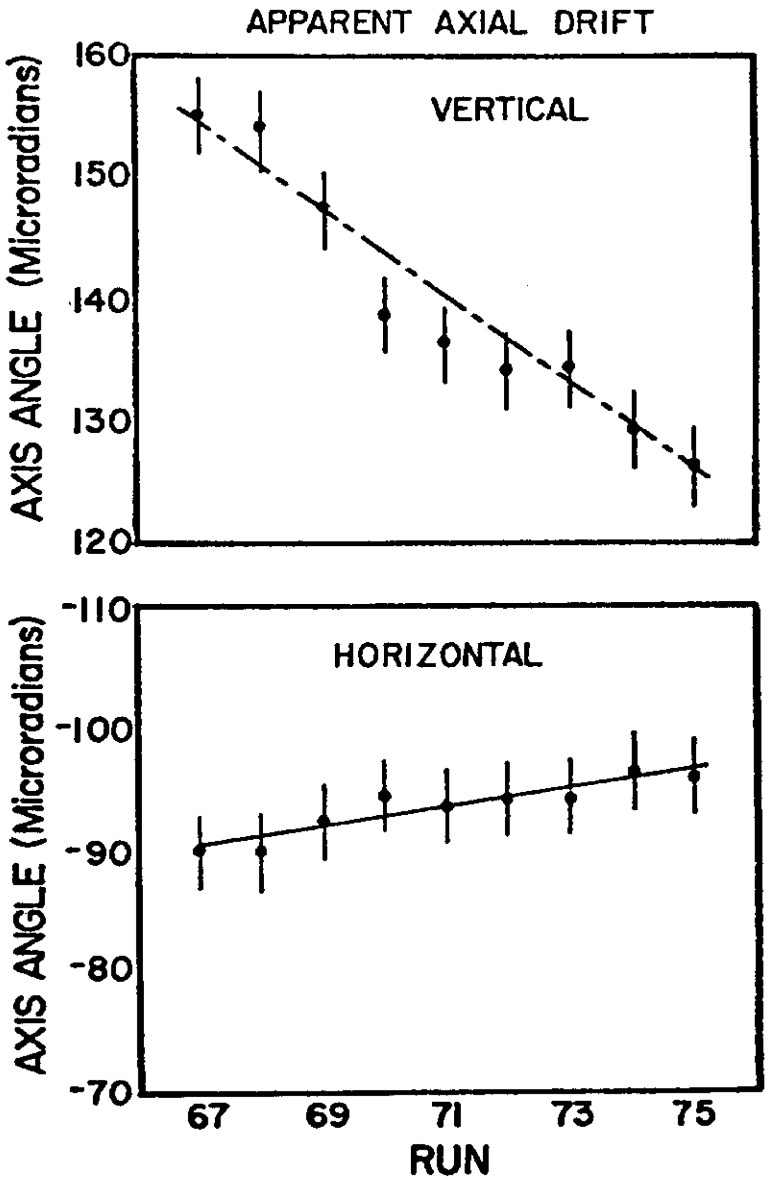
APPARENT AXIAL DRIFT
VERTICAL
HORIZONTAL
AXIS ANGLE (Microradians)
AXIS ANGLE (Microradians)
160
150
140
130
120
-110
-100
-90
-80
-70
67
69
71
73
75
RUN

Fig. 3

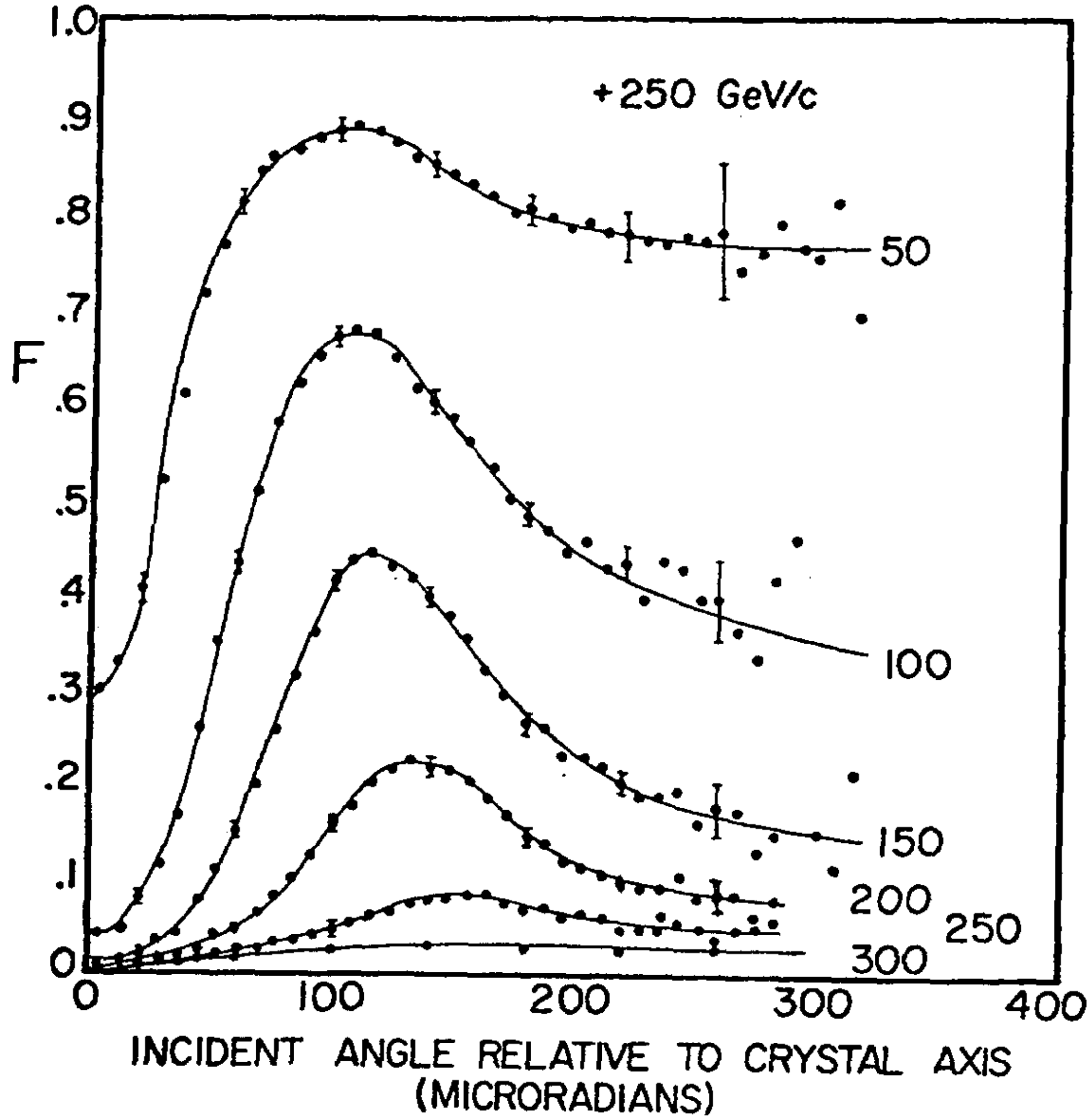
+250 GeV/c
F
1.0
.9
.8
.7
.6
.5
.4
.3
.2
.1
0
50
100
150
200
250
300
0
100
200
300
400
INCIDENT ANGLE RELATIVE TO CRYSTAL AXIS
(MICRORADIANS)

Fig. 4

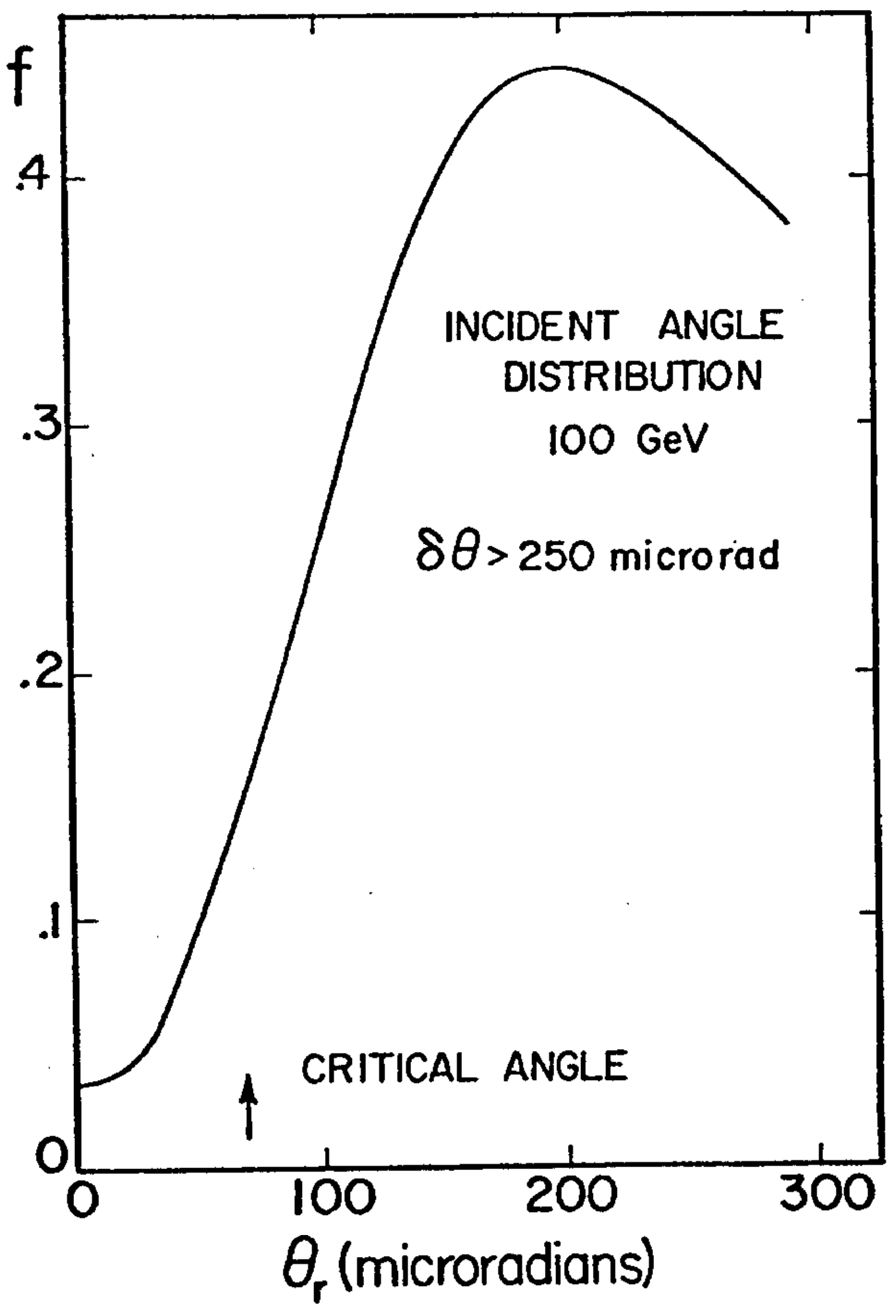
f
.4
.3
.2
.1
0
0
100
200
300
θ_r (microradians)
INCIDENT ANGLE DISTRIBUTION
100 GeV
$\delta\theta > 250$ microrad
CRITICAL ANGLE

Fig. 5

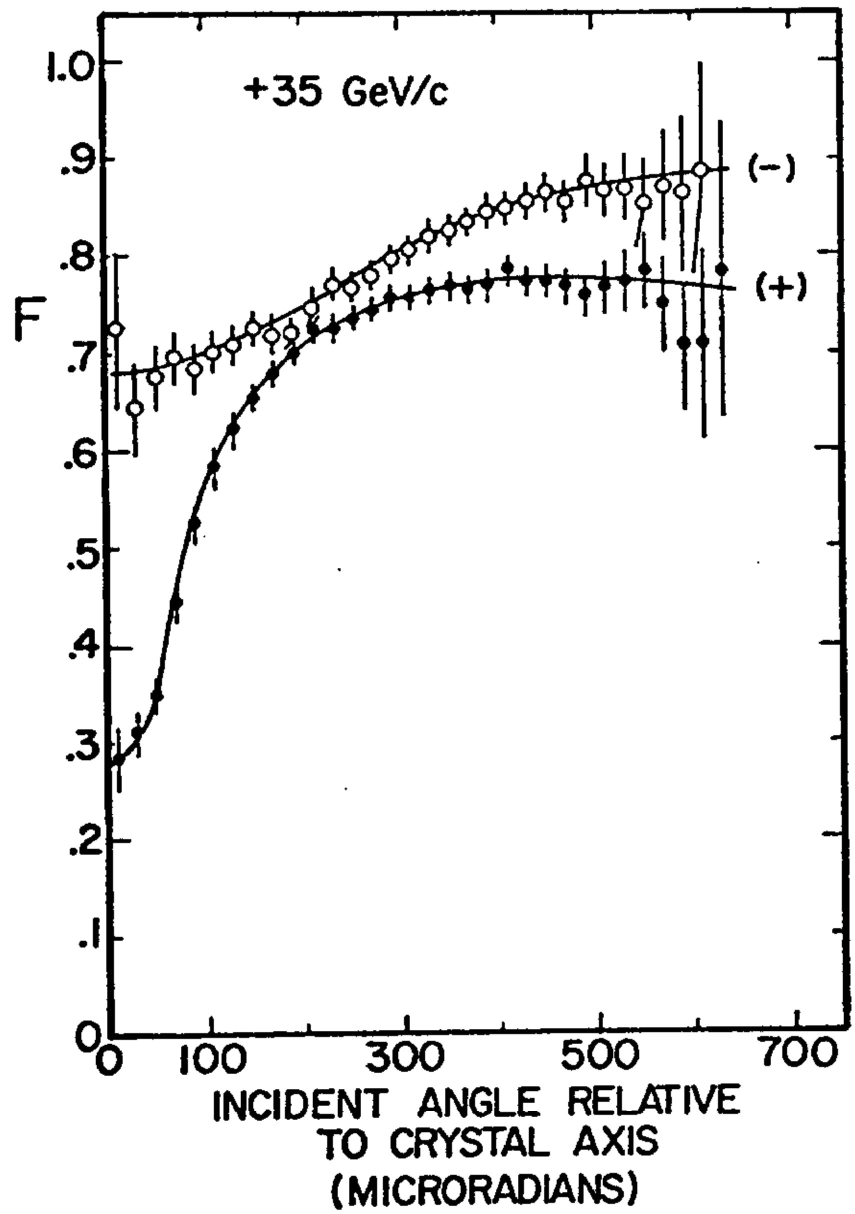
+35 GeV/c
1.0
.9
.8
.7
.6
.5
.4
.3
.2
.1
0
F
(−)
(+)
0
100
300
500
700
INCIDENT ANGLE RELATIVE
TO CRYSTAL AXIS
(MICRORADIANS)

Fig. 6

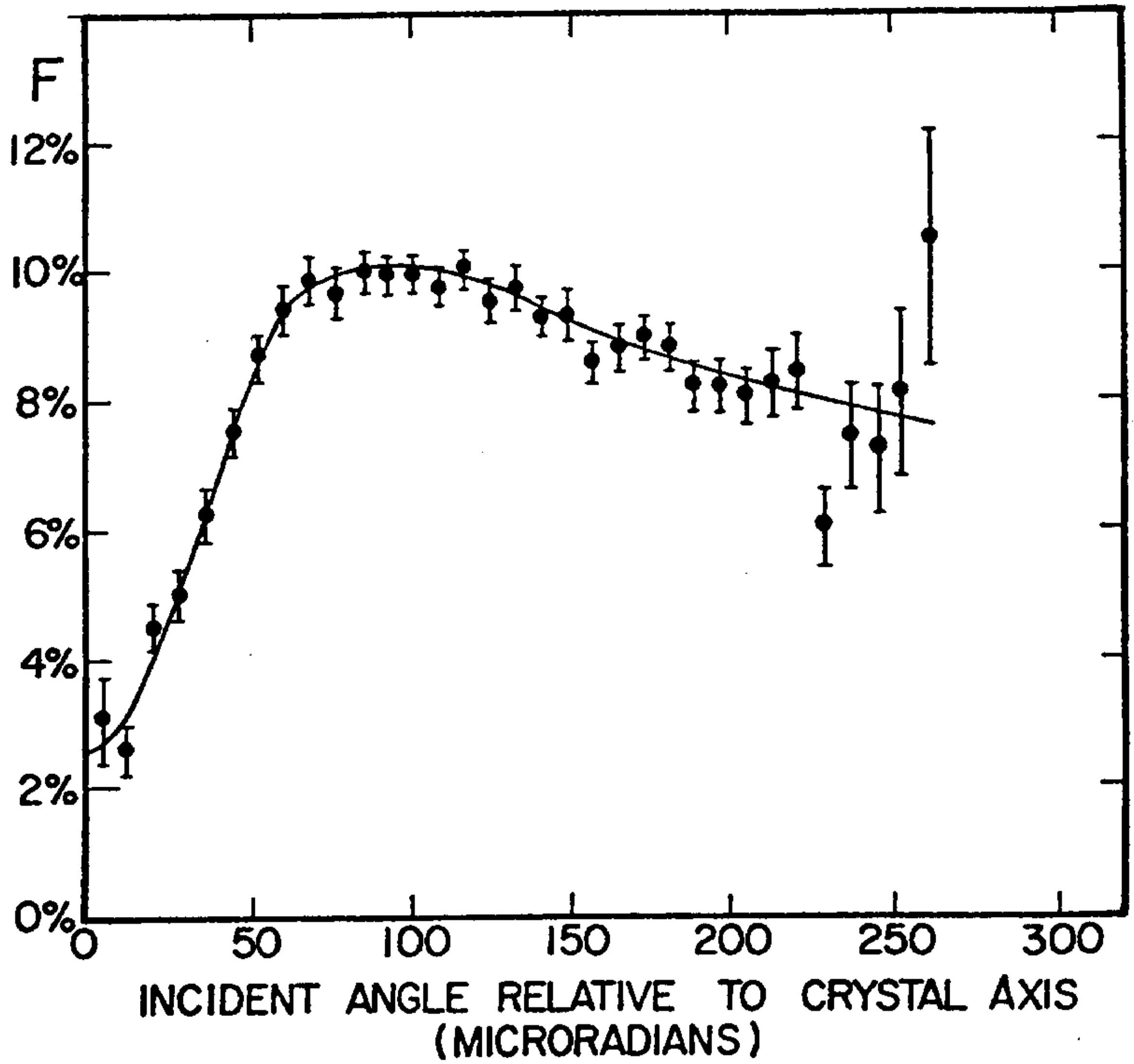
F
12%
10%
8%
6%
4%
2%
0%
0
50
100
150
200
250
300
INCIDENT ANGLE RELATIVE TO CRYSTAL AXIS
(MICRORADIANS)

Fig. 7

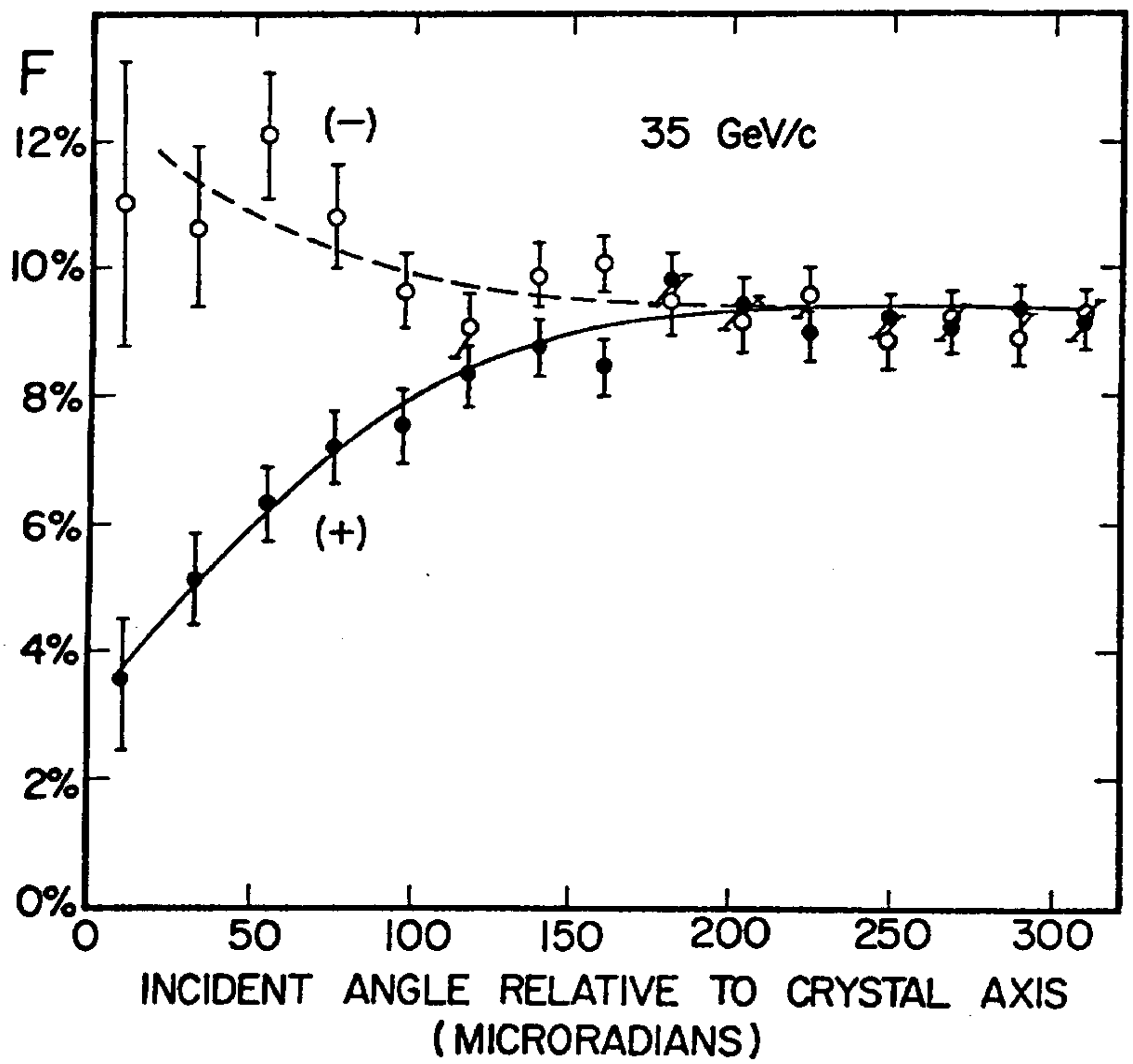
F
12%
10%
8%
6%
4%
2%
0%
(−)
(+)
35 GeV/c
0
50
100
150
200
250
300
INCIDENT ANGLE RELATIVE TO CRYSTAL AXIS
(MICRORADIANS)

Fig. 8

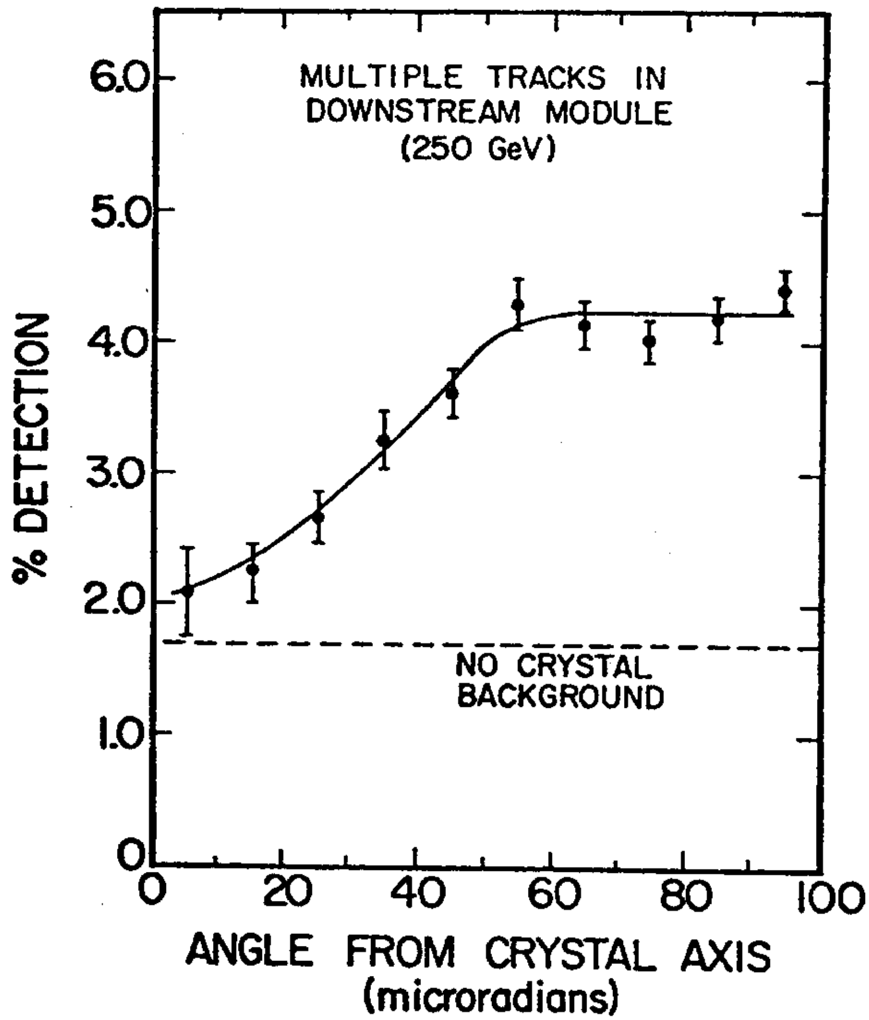
MULTIPLE TRACKS IN
DOWNSTREAM MODULE
(250 GeV)
6.0
5.0
4.0
3.0
2.0
1.0
0
% DETECTION
NO CRYSTAL
BACKGROUND
0
20
40
60
80
100
ANGLE FROM CRYSTAL AXIS
(microradians)

Fig. 9